Thermodynamic analysis of growth of iron oxide films by MOCVD using tris(*t*-butyl-3-oxo-butanoato)iron(III) as precursor

SUKANYA DHAR*, K SHALINI and S A SHIVASHANKAR

Materials Research Centre, Indian Institute of Science, Bangalore 560 012, India

Abstract. Thermodynamic calculations, using the criterion of minimization of total Gibbs free energy of the system, have been carried out for the metalorganic chemical vapour deposition (MOCVD) process involving the β-ketoesterate complex of iron [tris(*t*-butyl-3-oxo-butanoato)iron(III) or Fe(tbob)$_3$] and molecular oxygen. The calculations predict, under different CVD conditions such as temperature and pressure, the deposition of carbon-free pure Fe$_3$O$_4$, mixtures of different proportions of Fe$_3$O$_4$ and Fe$_2$O$_3$, and pure Fe$_2$O$_3$. The regimes of these thermodynamic CVD parameters required for the deposition of these pure and mixed phases have been depicted in a 'CVD phase stability diagram'. In attempts at verification of the thermodynamic calculations, it has been found by XRD and SEM analysis that, under different conditions, MOCVD results in the deposition of films comprising pure and mixed phases of iron oxide, with no carbonaceous impurities. This is consistent with the calculations.

Keywords. MOCVD; pure and mixed iron oxide films; CVD phase stability diagrams.

1. Introduction

Iron oxide thin films have found widespread application as materials for gas sensors, protecting pigments, magnetic recording media, and catalysis, because of their high thermal stability, hardness, and favourable magnetic properties (Mathur *et al* 2002). As one of the most powerful techniques suitable for the formation of stoichiometric and microstructured thin films (Park *et al* 2006), chemical vapour deposition has been employed for fabrication of iron oxide thin films from different precursors (Shalini *et al* 2003 and the references therein; Mathur *et al* 2006; Park *et al* 2006; Pflitsch *et al* 2006; Lee *et al* 2007). The overall motivation for the present work has been to conduct analytical studies to provide stability windows in the CVD process employing metalorganic precursors, corresponding to the experimental realization of specific iron oxide phases.

As CVD is by definition a chemical process, various process parameters and chemistry of the precursor affect the formation of a given phase, its microstructure, and related properties. Thermodynamic analysis of chemical reactions has been employed extensively to design and optimize chemical processes (engineering). Such analysis has also been occasionally applied to the development and understanding of CVD, assuming that equilibrium prevails in the process, which is applicable when the rate of deposition is low (Stringfellow 1989; Bernard *et al* 1999; Kang

et al 2000). For the CVD of transition metal oxides with multiple oxidation states, thermodynamic calculations can be employed to infer the deposition conditions required to obtain specific oxide phases. These conditions include the (substrate) temperature, the pressure in the CVD reactor, and the relative molar concentration of the reactants.

A β-ketoesterate complex, viz. tris(*t*-butyl-3-oxo-butanoato)iron(III), abbreviated as Fe(tbob)$_3$, was used in the present study as precursor, because of the enhanced volatility caused by the oxygen atom in the terminal group of this subliming solid (molecular structure shown in figure 1). It is a natural precursor for the CVD of oxide films, because each metal–ion is bonded directly to six oxygen-ions in each molecule. It may be expected that complexes of this type, when used as precursor under different sets of CVD process parameters, may yield the metal or dif-
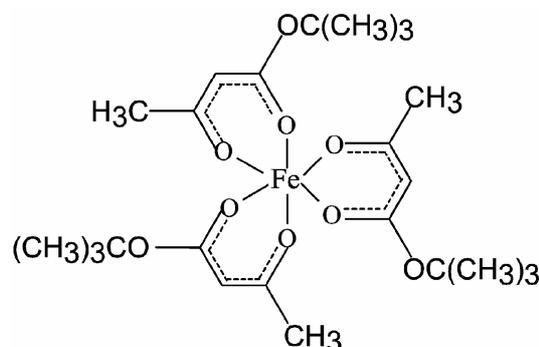

Figure 1. Molecular structure of the metalorganic complex, Fe(tbob)$_3$.

*Author for correspondence (sukanya@mrc.iisc.ernet.in)

Table 1. Phases considered for the thermodynamic analysis of MOCVD in oxygen atmosphere.

Solid	Fe, $Fe_{0.945}O$, $Fe_{0.947}O$, FeO, $FeO_{1.056}$, $FeO_{1.5}$, Fe_3O_4, Fe_2O_3, $Fe(OH)_2$, $Fe(OH)_3$, $Fe_2O_3.H_2O$, FeO.OH, Fe_3C, $FeCO_3$, C
Gaseous	CO, CO_2, H_2O, C_4H_8 (2-methyl propene, or isobutene), C_2H_2O (ketene), CH_3CHO (acetaldehyde), HCOOH (formic acid), and CH_3COOH (acetic acid)

ferent oxides of the multivalent metal, or various combinations of these components with carbon, as observed in the case of copper (Ottosson and Carlsson 1996; Mukhopadhyay *et al* 2002a, b) and cobalt metalorganic complexes (Paranjape *et al* 2002; Mane and Shivashankar 2003; Apátiga and Castaño 2006).

Equilibrium compositions of the solid and gaseous species formed during the deposition process have been calculated for a relatively high flow rate of oxygen, as functions of several CVD parameters. This leads to the construction of 'CVD stability diagrams', which have been verified by carrying out experiments designed for the purpose. Thus, iron oxide films were deposited at different substrate temperatures (T_{sub}), total reactor pressures (P), and at various flow rates of oxygen (F_{oxy}). The phase compositions and microstructure of the films deposited were studied using X-ray diffraction (XRD) and scanning electron microscopy (SEM), respectively.

2. Procedure

2.1 *Analytical*

The method of equilibrium calculations is based on the minimization of the Gibbs free energy of the system considered, satisfying the mass balance conditions (Eriksson 1971). The approach requires the identification of all the possible reactants and reaction products. The procedure for enumerating the gaseous species to be considered in the calculations, by consulting the mass spectrum of the precursor and employing 'chemical reasoning', is described in our earlier publications (Mukhopadhyay *et al* 2002a, b; Dhar *et al* 2008). For the CVD process with $Fe(tbob)_3$ as precursor, every possible solid product was considered for the analytical study. These are listed in table 1, along with the possible gaseous products. Calculations were performed, as described earlier (Mukhopadhyay *et al* 2002a, b; Dhar *et al* 2008), to obtain the concentrations of the various possible solid and gaseous products of the MOCVD process, as functions of substrate temperature (T_{sub}), total reactor pressure (P), and the ratio of the molar flow rates of oxygen and the vapour of the metalorganic precursor (O_2/Pre). The corresponding phase stability diagrams were also constructed.

2.2 *Experimental*

The iron complex was synthesized, purified, and characterized in house (Urs *et al* 2000). Iron oxide thin films

were grown on glass substrates in a hot-wall, horizontal, low-pressure MOCVD reactor, in which the total pressure (P), flow rates of carrier (argon) and reactant (oxygen) gases, substrate temperature (T_{sub}), and the precursor vapourizer temperature (T_{vap}), could be controlled. While electronic mass flow controllers were used to regulate the flow of the gases, the average flow rate of the vapours of the metalorganic precursor was computed from the weight loss of the precursor during a deposition run, assuming the vapour to be a perfect gas. Further details of the CVD process are described elsewhere (Shalini *et al* 2003). The as-deposited films were characterized by X-ray diffraction (XRD) for the identification of crystalline phases, and scanning electron microscopy (SEM) for morphology.

3. Results and discussion

3.1 *Analytical*

As already noted, an important variable in thermodynamic calculations is the relative molar concentrations of the reactants, i.e. molar flow rates of oxygen, and the metalorganic complex, in the present case. While this molar ratio, O_2/Pre, may be varied over a wide range experimentally, there is an upper limit to the number of moles of oxygen that can be consumed by one mole of the precursor. This is the number of moles of oxygen required to oxidize all the constituent atomic species completely. This limit is 30 for $Fe(tbob)_3$, based on the assumption of complete oxidation of Fe, C, and H to Fe_2O_3, CO_2, and H_2O, respectively. The presence of oxygen beyond this limit does not affect the thermodynamic calculations, though, in the actual deposition process, this extra oxygen may change the hydrodynamics of the CVD system. The range of O_2/Pre ratios used in this analytical study is close to the upper limit, and the same range was employed in the experimental deposition process.

Figure 2 shows variations in the calculated equilibrium molar concentrations of various condensed phases, as functions of O_2/Pre, at $T_{sub} =$ (a) 350°C and (b) 500°C, and $P = 2$ Torr. All calculations have been carried out assuming that one mole of the precursor is consumed. (If the amount of precursor consumed is different, the numbers on the ordinate of figure 2 will be altered merely by a multiplication factor, the relative proportions of the compounds formed remaining the same). At 350°C (figure 2(a)), simultaneous deposition of Fe_3O_4 (magnetite) and carbon (on the substrate) is to be expected for lower ratios of O_2/Pre, accompanied by carbon monoxide, carbon

dioxide, and water vapour in the gas phase. The amount of carbon in the deposit decreases with increasing O_2/Pre ratio, and finally reduces to zero, resulting in pure Fe_3O_4 films on a suitable substrate. At 500°C (figure 2(b)), no carbon impurity is to be expected in the deposit of Fe_3O_4 that occurs in the range of O_2/Pre ratios considered for the present study (26–32). At both these temperatures, as the O_2/Pre ratio is increased further, the deposition of pure Fe_3O_4 is accompanied by the formation of a significantly rising amount of CO_2 and a correspondingly diminishing amount of CO. This continues till the number of moles of CO formed becomes zero, while that of CO_2 reaches its maximum. When O_2/Pre is increased beyond this point, the additional oxygen contributes to the formation of increasing proportions of the higher oxide, Fe_2O_3 (α-Fe_2O_3, or hematite), resulting in a mixture of Fe_3O_4 and Fe_2O_3 in the condensed phase. It is interesting to note that pure Fe_2O_3 is not expected in the solid phase until the com-

plete oxidation of CO in the gas phase. Pure Fe_2O_3 in the solid phase, and CO_2 and H_2O in the gas phase, are expected when the O_2/Pre ratio reaches its maximum value of 30, beyond which there is no change in the relative proportion of these chemical species.

Results of similar calculations, performed as a function of T_{sub}, are summarized by constructing a CVD phase-stability diagram to represent the formation of solid phases (figure 3). The boundary lines separating the regimes of pure Fe_3O_4, mixture of Fe_3O_4 and Fe_2O_3, and pure Fe_2O_3, are found to be essentially invariant with temperature. The composition of the mixture, resulting from a simultaneous deposition of the two oxides, is also essentially independent of temperature (the proportion of Fe_2O_3 in the mixture increases extremely slowly with temperature). However, the O_2/Pre ratio required for the elimination of carbon from the deposit decreases as the temperature is increased. That is, the process window for the deposition of carbon-free pure Fe_3O_4 films becomes wider at higher deposition temperatures. It is noteworthy that, although the CVD stability diagram is constructed for a process very different from the elemental Fe–O system considered in 'traditional' binary phase diagrams, regions of stability exist in which more than one oxide phase is present, just as in the Fe–O binary phase diagram.

Confusion may arise at a first glance of figure 3 because, without the gaseous species also being represented, the equilibrium CVD diagram looks like the familiar Fe–O binary system (Kingery *et al* 1976), to which it is not expected to be equivalent. The binary Fe–O phase diagram represents analysis carried out for pairs of iron oxide systems, and each boundary line corresponds to a reaction of the type $Fe_3O_4 + O_2 \rightarrow Fe_2O_3$, carried out at one atmospheric pressure. In the case of CVD, a particular precursor, with its own specific constraint of elemental composition and molecular structure, reacts with oxygen, typically at a
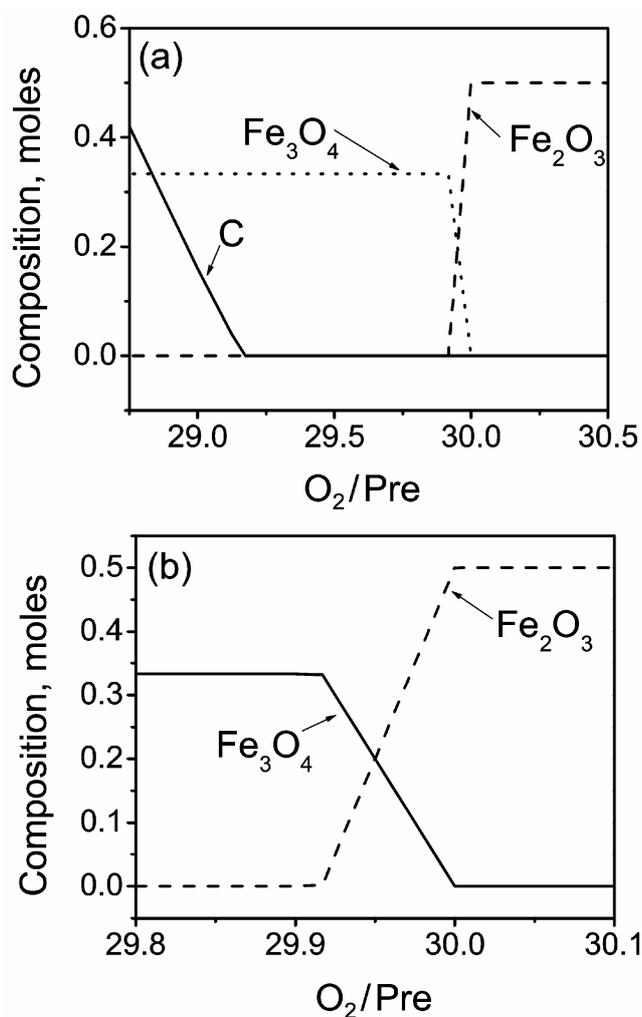

Figure 2. Variations in the calculated equilibrium molar concentrations of various condensed phases as a function of O_2/Pre ratio, at P = 2 Torr, and T_{sub} = (a) 350°C and (b) 500°C.
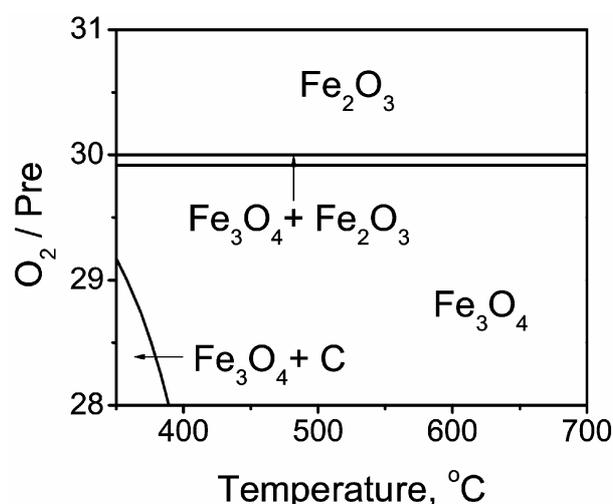

Figure 3. A 'CVD phase stability diagram' for solid phase formation, as a function of substrate temperature at P = 2 Torr.

reduced pressure. As the temperature and the O_2/Pre ratio are varied, reactions taking place along different chemical pathways to produce several condensed and gaseous products, are in equilibrium. The formation of the gaseous species, CO, CO_2, and H_2O, along with different oxides of iron, is an integral part of the MOCVD process. The boundaries in these CVD stability diagrams do not correspond to any particular reaction of the kind mentioned above regarding the binary Fe–O phase diagram. The CVD stability diagram separates regions of different pure and mixed phases, and points to the formation of different phases in different parts of the parameter space. Nevertheless, this phase stability diagram is in qualitative agreement with the phase diagram presenting the stability ranges for the oxides of iron, determined experimentally by reactive vapour deposition method (Fujii *et al* 1989).

As a function of another CVD parameter, viz. the reactor pressure, the CVD stability diagram for solid phase formation (figure 4) again presents trends similar to those described above. The O_2/Pre ratios corresponding to the boundaries between pure Fe_3O_4, the mixed phase, and pure Fe_2O_3, are found to be constant, irrespective of pressure, while the region of formation of Fe_3O_4 accompanied by C widens, with increasing pressure. Compositions of the simultaneously deposited oxides are independent of pressure as well.

3.2 *Experimental*

MOCVD runs were carried out using process parameters spanning the range suggested by the thermodynamic analysis. The ranges of substrate temperature and total reactor pressure required for measurable deposition were consistent with thermodynamic analysis, while the O_2/Pre ratio had to be raised by different amounts above the
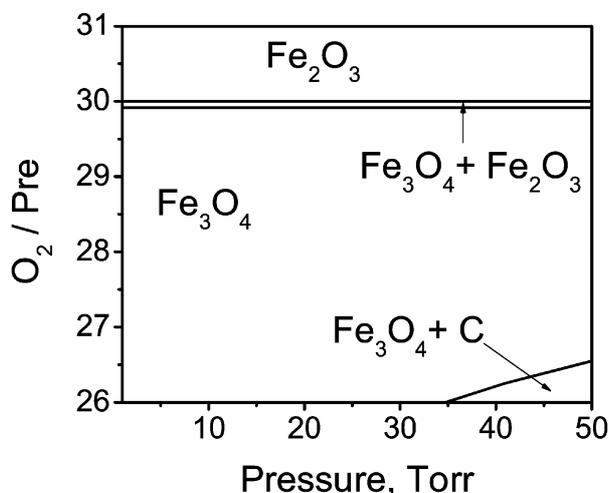
theoretically suggested values to obtain films of required compositions (which are different pure and mixed oxide phases, without much carbon impurity). Pure Fe_3O_4 was obtained for F_{oxy} = 50 sccm and 100 sccm, which corresponds to experimental O_2/Pre ratios of 29·8 and 35·5. However, Fe_3O_4 was deposited simultaneously with Fe_2O_3 at F_{oxy} = 150 sccm (corresponding O_2/Pre = 41·1), and pure Fe_2O_3 was deposited at F_{oxy} = 200 sccm (corresponding O_2/Pre = 47·4). This discrepancy between experiments and thermodynamic analysis in the required O_2/Pre ratio may be due to kinetic factors, such as the relative sticking probabilities of the molecules of oxygen and the precursor on the substrate (Kang *et al* 2000). It may also be due to progressive reduction in the residence time of the precursor as the total gas flow rate is raised holding the total reactor pressure constant at 2 Torr. In this case, the proportion of oxygen, which actually gets adsorbed on the substrate surface and reacts with the precursor during deposition, may be much smaller than the supplied quantity, thus accounting for the requirement of a much larger O_2/Pre ratio. The need for and the extent of higher O_2/Pre ratio (than that given by calculations) may also depend in part on hydrodynamics, i.e. the specific design of the reactor.

The dependence of iron oxide phase formation on the oxygen flow rate, for films grown at constant substrate temperature and total reactor pressure, is clearly seen in the XRD patterns (figure 5). The films do not show any
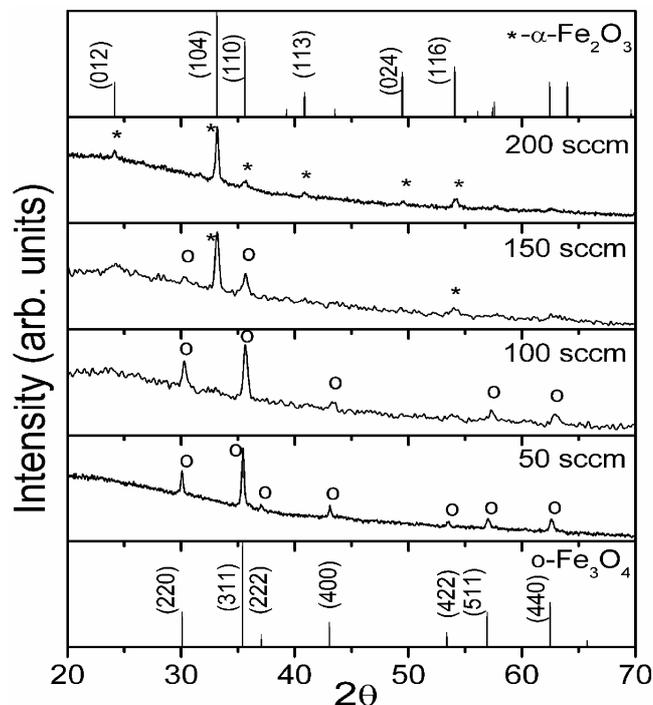

Figure 4. A 'CVD phase stability diagram' for solid phase formation, as a function of reactor pressure, at T_{sub} = 500°C.

Figure 5. XRD patterns of iron oxide films deposited for oxygen flow rate (F_{oxy}) ranging from 50 sccm to 200 sccm, at T_{sub} = 500°C and P = 2 Torr.
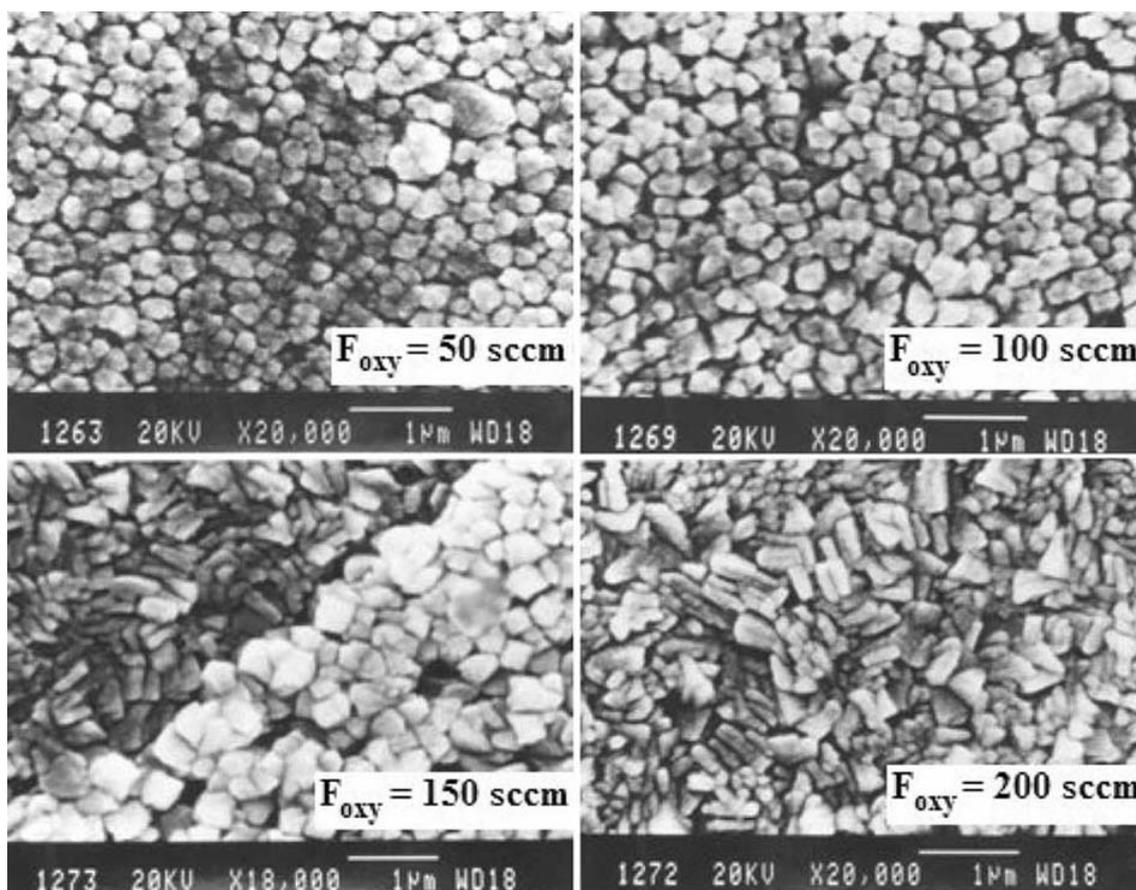
Figure 6. SEM micrographs corresponding to films presented in figure 5.

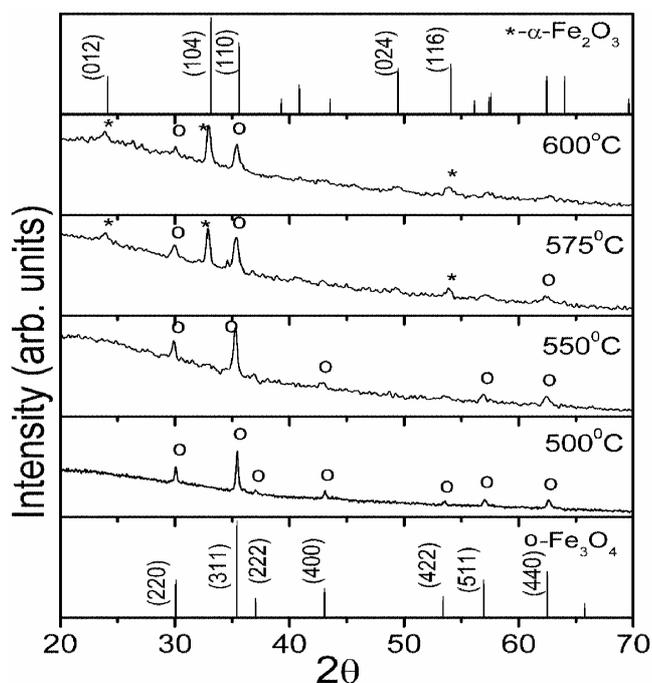**Figure 7.** XRD patterns of iron oxide films deposited at temperatures in the range 500–600°C, for F_{oxy} = 50 sccm and P = 2 Torr.

crystallographic texture at the deposition (substrate) temperature of 500°C. At T_{sub} = 500°C, P = 2 Torr, and oxygen flow rate (F_{oxy}) ranging from 20–100 sccm, the only phase formed is Fe_3O_4. Peaks corresponding to α-Fe_2O_3, along with those corresponding with Fe_3O_4, are present in the film deposited when the oxygen flow rate is increased to 150 sccm, implying simultaneous deposition of the two oxides at the higher O_2/Pre ratio employed. The intensity of the α-Fe_2O_3 peaks, indicative of the amount of α-Fe_2O_3 in the films, increases with increased flow rate of oxygen. Finally, when the oxygen flow rate is 200 sccm, pure, polycrystalline α-Fe_2O_3 is formed, in accordance with the thermodynamic predictions. The changeover from Fe_3O_4 to α-Fe_2O_3 phase is clearly illustrated by the differing morphology of the two phases, as seen by SEM (figure 6).

It is interesting to note that the XRD patterns follow a trend similar to that in figure 5, when iron oxide films were deposited at different temperatures in the range 500–600°C, while reactor pressure and oxygen flow rate are held constant at 2 Torr and 20 sccm, respectively (figure 7). Pure Fe_3O_4 is formed up to 550°C, and a combination of Fe_3O_4 and α-Fe_2O_3 at higher temperatures. The corresponding SEM patterns also clearly indicate the existence of pure and mixed phases (Shalini *et al* 2003), displaying the distinct morphologies of the crystallites of Fe_3O_4 and
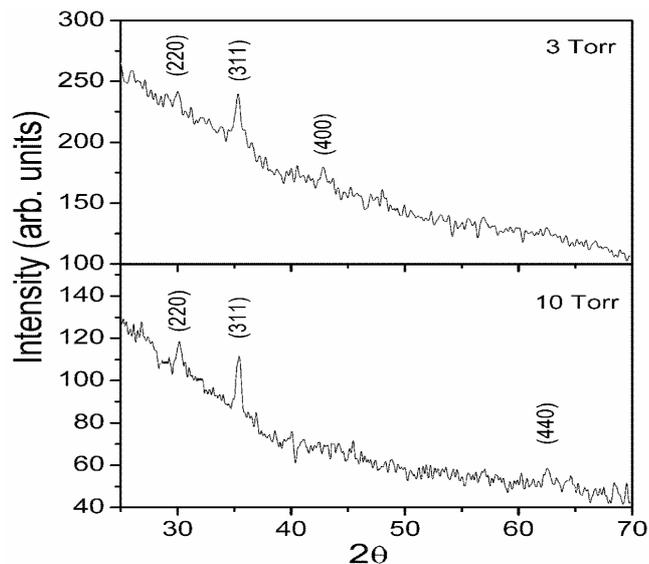
Figure 8. XRD patterns of Fe_3O_4 films deposited at different pressures, keeping the substrate at 500°C and the oxygen flow at 50 sccm.

α-Fe_2O_3. The experimental results indicate a strong dependence of the phase composition of the films on temperature, in contrast with the theoretical calculations. It may be inferred that the actual O_2/Pre ratio at the growth surface increases with increasing temperature because of the dependence of the adsorption kinetics of the reactants on temperature (Kang *et al* 2000). Therefore, an increase in deposition temperature is similar to an effective increase in the O_2/Pre ratio, pointing to a qualitative agreement between the theoretical predictions and the experimental observations.

The characterization for the films grown at different pressures was restricted by the poor crystallinity and the falling growth rate of the films with increasing pressure (XRD patterns shown in figure 8). Increasing rates of gas phase reactions, which lead to a diminishing flux of reactants at the substrate surface, may cause the observed decline in the growth rate at higher reactor pressures, while simultaneous deposition of carbon (figure 4) may account for the poor crystallinity.

4. Summary and conclusions

Thermodynamic modeling of the MOCVD growth of iron oxide thin films, using the ketoesterate metalorganic complex, tris(*t*-butyl-3-oxo-butanoato)iron(III), as the precursor, was carried out. Concentrations of various solid and gaseous species expected to be formed under equilibrium conditions were computed as functions of CVD parameters, viz. substrate temperature, total reactor pressure, and the relative molar proportion of the metalorganic precursor and oxygen. The corresponding 'CVD phase stability diagrams' for the formation of the solid phases were constructed, indicating the process windows for the

formation of different phases. Experimental results are in qualitative agreement with the thermodynamic calculations, specifically including the prediction of the simultaneous formation of hematite (α-Fe_2O_3) and magnetite (Fe_3O_4) under certain deposition conditions. The quantitative discrepancy between calculated and experimental results may be attributed to the dependence of the actual O_2/Pre ratio at the growth surface on the deposition parameters. Thermodynamic calculations can, therefore, be useful in predicting trends in a MOCVD process involving metals with multiple oxidation states and, thus, be helpful in identifying possible impurities and/or undesired phases in the solid deposit.

Acknowledgement

References

Apátiga L M and Castaño V M 2006 *Thin Solid Films* **496** 576
Bernard C, Pons C M, Blanquet E and Madar R 1999 *MRS Bull.* **24** 27
Dhar S, Dharmaprakash M S and Shivashankar S A 2008 *Bull. Mater. Sci.* **31** 67
Eriksson G 1971 *Acta Chem. Scand.* **25** 651
Fujii T, Takano M, Katano R and Bando Y 1989 *J. Appl. Phys.* **66** 3168
Kang S Y, Choi K H, Lee S K, Hwang C S and Kim H J 2000 *J. Electrochem. Soc.* **147** 1161
Kingery W D, Bowen H K and Uhlmann D R 1976 *Introduction to ceramics* (New York: John Wiley and Sons)
Lee J Y, Kang B C, Jung D Y and Boo J H 2007 *J. Vac. Sci. Technol.* **B25** 151
Mane A U and Shivashankar S A 2003 *J. Crystal Growth* **254** 368
Mathur S, Veith M, Sivakov V, Shen H, Huch V, Hartmann U and Gao H B 2002 *Chem. Vap. Depos.* **8** 277
Mathur S, Sivakov V, Shen H, Barth S, Cavelius C, Nilsson A and Kuhn P 2006 *Thin Solid Films* **502** 88
Mukhopadhyay S, Shalini K, Lakshmi R, Devi A and Shivashankar S A 2002a *Surf. Coat. Technol.* **150** 205
Mukhopadhyay S, Shalini K, Devi A and Shivashankar S A 2002b *Bull. Mater. Sci.* **25** 391
Ottosson M and Carlsson J 1996 *Surf. Coat. Technol.* **78** 286
Paranjape M A, Mane A U, Raychaudhuri A K, Shalini K, Shivashankar S A and Chakravarty B R 2002 *Thin Solid Films* **413** 8
Park S, Lim S and Choi H 2006 *Chem. Mater.* **18** 5150
Pflitsch C, Viefhaus D, Bergmann U, Kravets V, Nienhaus H and Atakan B 2006 *J. Electrochem. Soc.* **153** C546
Shalini K, Subbanna G N, Chandrasekaran S and Shivashankar S A 2003 *Thin Solid Films* **424** 56
Stringfellow G B 1989 *Organometallic vapour phase epitaxy–theory and practice* (New York: Academic Press) Ch. 3
Urs U K, Shalini K, Dharmaprakash M S, Shivashankar S A and Row T N G 2000 *Acta Crystallogr.* **C56** e448